Impact of 2020 COVID-19 lockdowns on particulate air pollution across Europe

Jean-Philippe Putaud[1], Enrico Pisoni[1], Alexander Mangold[2], Christoph Hueglin[3], Jean Sciare[4], Michael Pikridas[4], Chrysanthos Savvides[5], Jakub Ondracek[6], Saliou Mbengue[7], Alfred Wiedensohler[8], Kay Weinhold[8], Maik Merkel[8], Laurent Poulain[8], Dominik van Pinxteren[8], Hartmut Herrmann[8], Andreas Massling[9], Claus Nordstroem[9], Andrés Alastuey[10], Cristina Reche[10], Noemí Pérez[10], Sonia Castillo[11], Mar Sorribas[12], Jose Antonio Adame[12], Tuukka Petaja[13], Katrianne Lehtipalo[13], Jarkko Niemi[14], Véronique Riffault[15], Joel F. de Brito[15], Augustin Colette[16], Olivier Favez[16], Jean-Eudes Petit[17], Valérie Gros[17], Maria I. Gini[18], Stergios Vratolis[18], Konstantinos Eleftheriadis[18], Evangelia Diapouli[18], Hugo Denier van der Gon[19], Karl Espen Yttri[20], Wenche Aas[20].

[1]European Commission, Joint Research Centre (JRC), Ispra, Italy.
[2]Scientific Service Observations, Royal Meteorological Institute of Belgium, Brussels, Belgium.
[3]Swiss Federal Laboratories for Materials Science and Technology (EMPA), Duebendorf, Switzerland.
[4]Climate and Atmosphere Research Center, The Cyprus Institute, Nicosia, 2121, Cyprus.
[5]Ministry of Labour and Social Insurance, Department of Labour Inspection (DLI), Nicosia, Cyprus.
[6]Institute of Chemical Process Fundamentals, Czech Academy of Sciences, Prague, Czech Republic.
[7]Global Change Research Institute, Czech Academy of Sciences, Brno, Czech Republic.
[8]Atmospheric Chemistry Department (ACD), Leibniz Institute for Tropospheric Research (TROPOS), Leipzig, Germany.
[9]Department of Environmental Science, Aarhus University, Roskilde, Denmark.
[10]Institute of Environmental Assessment and Water Research (IDAEA-CSIC), Barcelona, 08034, Spain.
[11]Andalusian Institute for Earth System Research (IISTA-CEAMA), University of Granada, Granada, 18006, Spain.
[12]National Institute for Aerospace Technology (INTA), Mazaagón, Huelva, Spain.
[13]Institute for Atmospheric and Earth System Research INAR / Physics, University of Helsinki, Helsinki, Finland.
[14]Helsinki Region Environmental Services Authority (HSY), Helsinki, Finland.
[15]IMT Nord Europe, Institut Mines-Télécom, Univ. Lille, Centre for Energy and Environment, F-59000 Lille, France.
[16]Institut National de l'Environnement Industriel et des Risques, Verneuil-en-Hallate, France.
[17]Laboratoire des Sciences du Climat et de l'Environnement, Gif-sur-Yvette, France.
[18]Environmental Radioactivity & Aerosol Technology for Atmospheric & Climate Impact Lab, N.C.S.R. "Demokritos", 15341 Ag. Paraskevi, Attiki, Greece.
[19]TNO, Dept. Climate, Air and Sustainability, Utrecht, The Netherlands.
[20]NILU – Norwegian Institute for Air Research, P.O. Box 100, 2027 Kjeller, Norway.

Correspondence to: J.P. Putaud (jean.putaud@ec.europa.eu)

Abstract. To fight against the first wave of Coronavirus disease 2019 (COVID-19) in 2020, lockdown measures were implemented in most European countries. These lockdowns had well-documented effects on human mobility. We assessed the impact of the lockdown implementation and relaxation on air pollution by comparing daily particulate matter (PM), nitrogen dioxide (NO_2), and ozone (O_3) concentrations, as well as particle number size distributions (PNSD) and particle light absorption coefficients in-situ measurement data with values expected if no COVID-19 epidemic had occurred at 28 sites across Europe for the period 17 February – 31 May 2020. Expected PM, NO_2 and O_3 concentrations were calculated from the 2020 Copernicus Atmospheric Monitoring Service (CAMS) Ensemble forecasts, combined with 2019 CAMS Ensemble forecasts and measurement data. On average, lockdown implementations did not lead to a decrease in $PM_{2.5}$ mass concentrations at urban sites, while relaxations resulted in a $+26 \pm 21\%$ rebound. The impacts of lockdown implementation and relaxation on NO_2 concentrations were more consistent (-29 ± 17 %, and $+31 \pm 30$ %, respectively). The implementation of the lockdown measures also induced statistically significant increases in O_3 concentrations at half of all sites ($+13$ % on average). An enhanced oxidizing capacity of the atmosphere could have boosted the production of secondary aerosol at those places. By comparison with 2017 – 2019 measurement data, a significant change in the relative contributions of wood and fossil fuel burning to the concentration of black carbon during the lockdown was detected at 7 out of 14 sites. The contribution of particles smaller than 70 nm to the total number of particles significantly also changed at most of the urban sites, with a mean decrease of -7 ± 5 % coinciding with the lockdown implementation. Our study shows that the response of $PM_{2.5}$ and PM_{10} mass concentrations to lockdown measures was not systematic at various sites across Europe for multiple reasons, the relationship between road traffic intensity and particulate air pollution being more complex than expected.

1 Introduction

The first case of COVID-19 (Coronavirus disease 2019) in Europe was identified in Italy on 21 February 2020, although recent evidence suggests that the virus had already spread across northern Italy by mid-January (Cerqua and Di Stefano, 2022). National authorities took measures to limit the epidemics propagation across Europe and lockdown measures entered into force in various countries from March 2020. These measures led to dramatic decreases in activities such as road traffic (IEA, 2020), and large reductions in air pollutant emissions from these pollution sources were expected. Shortly after the first lockdown measures were implemented, numerous articles unsurprisingly reported about marked improvements in air quality across Europe (see examples in Putaud et al., 2021). These statements were mostly based on simple comparisons between 2020 and previous year data obtained from remote sensing or in-situ observations. Nonetheless, it was quickly shown that the impacts of the lockdown measures on air pollution were quite complex and could not be assessed without implementing sufficiently developed methodologies (Copernicus, 2020; Kroll et al., 2020; Shi et al., 2021; see also quotations in Schiermeier, 2020), including "deweathering" techniques (e.g. Goldberg et al., 2020; Petetin et al., 2020; Venter et al., 2020; Grange et al., 2021; Petit et al., 2021), modelling (Hammer et al., 2021; Yang et al., 2021) or combinations of model and measurement data (Le et al., 2020; Barré et al., 2021; Beloconi et al, 2021; Jiang et al., 2021). The latter were also applied by Putaud et al. (2021) to northern Italy, one of the most polluted areas in Europe, where the first major COVID-19 outbreak occurred in Europe. That work is extended here to about 30 urban and regional background sites across Europe, for which daily in-situ measurement data from February to May 2020 are compared to expected data (as if no COVID-19 epidemics had occurred) across the same period. The objectives of this work were (i) to determine the impact of the lockdown measures on particulate air pollution at urban and regional background sites across Europe, (ii) to discuss our findings after assessing the impact of the lockdown measures on key gaseous pollutants, on the aerosol light absorption spectrum and the shape of particle number size distributions (PNSD), and (iii) to study the relationship between these impacts and changes in human mobility during lockdowns across Europe. The consequences of the lockdown measures could give a hint on the impact of future car exhaust emission reductions on air pollution across Europe.

2 Material and methods

This study focuses on the COVID-19 lockdowns that occurred across Europe in spring 2020. For the sake of clarity, the same three periods were considered for all countries: a 3-week-period before lockdowns were implemented (A, "ante", 17 February – 8 March 2020), a 6-week period for which mobility was minimal across Europe (D, "during", 23 March – 3 May 2020), and a 3-week-period during which lockdown measures were partially or totally relaxed (P, "post", 11 – 31 May 2020). Therefore, the 2 week period 9 – 22 March is excluded from the analysis because lockdown measures were unevenly implemented across Europe at this time. Levels of

stringency during periods A, D, and P in the various countries are discussed in Section 3.1 on the basis of mobility data.

Measurements of particulate matter (PM_{10} and $PM_{2.5}$), nitrogen dioxide (NO_2), and ozone (O_3) surface level concentrations from 16 urban sites and 12 regional background sites located in 13 countries across Europe were examined for the three periods A, D and P. Measurement data from the same periods in 2019, together with model outputs for the same periods in both 2019 and 2020 were used to estimate the pollutant expected concentrations, which would have occurred in 2020 if no lockdown measures were applied. The potential impact of weather conditions on pollutant concentrations was therefore taken into account.

In addition to PM mass concentrations, two other variables characterising particulate air pollution were studied at 13 sites: (i) the Absorption Ångström exponent (AÅE), which describes the wavelength dependence of the particle light absorption coefficient and reflects the relative contributions of fossil fuel burning and wood burning to the atmospheric concentration of black carbon (Helin et al, 2021, and references therein), and (ii) the contribution of "small" particles (N_{small}) to the "total" number of particles (N_{tot}), as a proxy for primary particle emissions. Indeed, vehicle tail-pipe emissions have been shown to be dominated by particles whose mobility diameters (D_p) range between 15 and 70 nm (Giechaskiel et al, 2020; Garbariene et al., 2021). Wood combustion particle diameters are highly dependent on the combustion conditions. Particles with $D_p<70$ nm can also be emitted by wood burners (Hueglin et al., 1997). The growth of new particles produced during nucleation events also leads to particles in this size range. The number of particles in the size range 15 – 70 nm shall therefore be considered as an upper limit for the number of primary particles. Both variables AÅE and N_{small}/N_{tot} are intensive variables, i.e. they are not directly dependent on pollution dispersion and therefore much less sensitive to weather conditions than pollutant concentrations.

2.1 Mobility data

We could not find any statistical data whose time resolution was good enough (i.e. weekly or better) to assess lockdown impacts on human activities in a consistent way across all 13 countries considered in this study. Therefore, we focused on mobility data as proxies for lockdowns' stringencies. Driving route request data at city and regional scales temporarily made available by Apple® (Figure S1) at covid19.apple.com/mobility (last accessed 21/03/2022) were used as an indicator of road-traffic intensity for all sites, except those in Cyprus for which such data were not available.

To assess the relationship between Apple® driving route request data and the actual number of vehicle kilometres driven, monthly motor fuel consumption from EUROSTAT (ec.europa.eu/eurostat) and AVENERGY (www.avenergy.ch) from January to May 2020 were used. For Cyprus, monthly activity data from the national statistical service CYSTAT (www.cystat.gov.cy) were used.

2.2 Measurement sites

The 28 air pollution measurement sites considered in this study are shown in Figure 1. Details are listed in Table 1 where sites are sorted from North to South. Twenty-four of these sites constitute twin sites – 1 urban site and 1 regional background site in the same area (< 200 km).

2.3 Model data

We used CAMS (Copernicus Atmospheric Monitoring Service) Ensemble forecasts for PM_{10}, $PM_{2.5}$, NO_2, and O_3 daily surface level mass concentrations calculated as the median of the concentrations computed independently by nine different regional air quality models (Marecal et al., 2015), namely CHIMERE, DEHM, EMEP, EURAD-IM, GEM-AQ, LOTOS-EUROS, MATCH, MOCAGE, and SILAM. Each model is based on different schemes describing the formation, dispersion and deposition of reactive gases and particles, but uses the same meteorological fields from the ECMWF (European Centre for Medium-Range Weather Forecast) Integrated Forecasting System, and the same pollutant emission data derived from officially reported emissions for previous years, and therefore ignoring any potential lockdown effect (Denier van der Gon et al., 2015; Kuenen et al., 2022). The outputs of the nine individual models are interpolated on a common regular 0.1° x 0.1° latitude x longitude grid (about 10 km x 10 km) on 10 vertical levels from the surface layer (0-40 m) up to about 5 km altitude over Europe (defined as 25°W-45°E, 30°N-72°N). Median values are little sensitive to outliers (Riccio et al, 2007) and model ensembles are expected to yield better estimates than individual models (Galmarini et al., 2018).

2.4 Measurement data

2019 and 2020 PM_{10}, $PM_{2.5}$, NO_2, and O_3 measurement data from urban sites were collected from the local air quality monitoring networks, except for Athens, for which PM and NO_2 data originated from the ACTRIS (Aerosol, Clouds and Trace gases Research Infrastructure) Observatory operated by the National Centre for Scientific Research "Demokritos". Measurement data from regional background sites were also all produced by ACTRIS Observatories operated by research performing organisations or EMEP (co-operative programme for monitoring and evaluation of the long range transmission of air pollutants in Europe) monitoring sites, and provided by the ACTRIS Data Centre. Pollutant concentrations were measured from 3 to 9 m above the ground with methods listed in Tables S1 and S2 (Supplement).

PNSD and particle light absorption data from 2017 to 2020 originated from the authors' organisations. Data from ACTRIS sites were provided by the ACTRIS Data Centre, and data from other sites were specifically made available for this work. PNSD and particle light absorption coefficients were determined using instruments listed in Table S3.

2.5 Data analysis

Data were analysed as in Putaud et al., 2021. Briefly, 2020 expected daily concentrations (Exp_{2020}) were estimated from 2020 CAMS-Ensemble daily forecasts ($CAMS_{2020}$) and the ratio between 2019 daily observations (Obs_{2019}) and 2019 CAMS-Ensemble daily forecasts ($CAMS_{2019}$) according to Eq. 1:

$$Exp_{2020} = \frac{Obs_{2019}}{CAMS_{2019}} \, CAMS_{2020} \tag{1}$$

2020 CAMS–Ensemble forecasts account for actual meteorological conditions and seasonal changes in emission source strengths, ignoring lockdown measures. The ratio $Obs_{2019}/CAMS_{2019}$ represents the time dependent normalisation of CAMS forecasts to the observations performed at each measurement site, as estimated from 2019 data. Applying this normalisation factor to CAMS 2020 forecasts aims at correcting for the bias between CAMS forecasts and observation data, which can vary across the year. It should be noted that only sites for which forecasts and observations reasonably agreed ($R^2 \geq 0.5$) across February – May 2019 were considered in this study (see Table S4). Obviously, expected concentrations (Exp_{2020}) cannot be compared to observations (Obs_{2020}) on a daily basis, since Exp_{2020} values are affected by random variations in the daily $Obs_{2019}/CAMS_{2019}$ ratio. Instead, mean Obs_{2020}/Exp_{2020} ratios were compared for the 3 periods A (before lockdowns), D (during lockdowns), and P (after lockdowns), as defined in Section 2. The statistical significance of the difference in Obs_{2020}/Exp_{2020} ratios between the 3 time periods A, D, and P was assessed by applying a 2-sided t test to the averages $\bar{A}$, $\bar{P}$, and $\bar{D}$, defined as:

$$\bar{A} = mean\left(log\frac{Obs_{2020}}{Exp_{2020}}\right)_A, \bar{D} = mean\left(log\frac{Obs_{2020}}{Exp_{2020}}\right)_D, \bar{P} = mean\left(log\frac{Obs_{2020}}{Exp_{2020}}\right)_P \tag{2}$$

The null hypotheses ($\bar{D} = \bar{A}$ and $\bar{D} = \bar{P}$) were tested at the 95% confidence assuming unequal variances.

The mean Obs_{2020}/Exp_{2020} ratios plotted and discussed below were calculated as:

$$\langle A \rangle = 10^{\bar{A}}, \langle D \rangle = 10^{\bar{D}}, \text{ and } \langle P \rangle = 10^{\bar{P}} \tag{3}$$

Particle light absorption Ångström exponent (AÅE) values were calculated as the slope of the linear regression between the logarithm of the particle light absorption coefficients and the logarithm of the wavelengths (WL) of the light sources used in the multi-wavelength absorption photometers across the whole WL range available below 900 nm. WL ranges were different across the various sites (Table S3) but constant at each site. AÅE values were calculated across the ultraviolet – near infrared range (370 – 880 nm) for the urban sites in Lille (FR), Bern (CH), Athens (GR), Nicosia (CY) and the regional background sites SIR (FR), PAY (CH), IPR (IT) and MSY (ES). At Brussels (BE), measurements were available at 370 and 660 nm, and at ARN (ES), HYY (FI) and KOS (CZ), in the visible range (470 – 660 nm) only.

The ratio between the number of small particles (N_{small}) and the "total" number of particles (N_{tot}) was calculated from PNSD measurements. N_{small} was calculated by integrating PNSD from 15 to 70 nm at all sites, except Copenhagen and RIS (DK), for which PNSD lower bound was 41 nm. N_{tot} was calculated by integrating PNSDs from 15 nm to the upper bound of the distribution at all but both sites in Denmark (41 nm). The upper bound was 800 nm at most but not all sites (Table S3), and was constant at each site across the time period 2017 -2020.

Particle light absorption coefficients and PNSDs are not computed by the CAMS model. Therefore, 2017 – 2019 measurement data were used to calculate the expected values of the Absorption Ångström exponent (AÅE) and the contribution of small particles to the total particle number concentration (N_{small} / N_{tot}) for sites at which measurements were available for at least 2 years between 2017 and 2019 across the studied period (17 February – 31 May). Both being intensive variables (i.e. intrinsic aerosol properties), these variables are much less sensitive to weather conditions than e.g. atmospheric concentrations. Daily values expected for 2020 (Exp_{2020}) were calculated as the average of 2017 – 2019 data, and lockdowns' impacts were assessed comparing the arithmetic means of Obs_{2020}/Exp_{2020} ($\bar{A}$, $\bar{P}$, and $\bar{D}$) for the 3 time periods A, D, and P, as described above.

The mean impact of the lockdown implementation and relaxation discussed below and listed in Table 2 were calculated for each variable as:

$$\text{lockdown implementation mean impact} = \frac{1}{n}\sum_{i=1}^{n}(\langle A_i\rangle/\langle D_i\rangle - 1) \qquad (4a)$$

and $\quad$ $$\text{lockdown relaxation mean impact} = \frac{1}{n}\sum_{i=1}^{n}(\langle D_i\rangle/\langle P_i\rangle - 1) \qquad (4b)$$

where indices $(1, \dots, n)$ represent the sites considered for each variable. Mean impacts were expressed as percentages (%).

3 Results and discussion

3.1 Impact of lockdown measures on road traffic intensity

Biases in traffic intensity estimates derived from mobility data have been reported in business as usual conditions (Meppelink et al., 2020). However, data relative to the lockdown period in the USA have highlighted a clear covariation between Apple® mobility data and gasoline demand (Ou et al., 2020), which is in turn a robust indicator for the cumulative distance covered by cars. We compared monthly mean motor fuel consumptions and Apple® driving direction requests for the 12 countries of this study for which data were available. Table S5 shows that gasoline national consumptions are generally well correlated with country mean driving direction requests across January – May 2020, while diesel consumptions are anti-correlated or not-significantly correlated with driving direction requests in all countries but 3 (FR, IT, ES). This suggests that Apple® driving direction requests are good qualitative proxies for personal car traffic but not for commercial (diesel powered) vehicular traffic. This is confirmed by data from Athens, for which a reduction between A and D of up to 70% and 40% in Light Duty Vehicle and Heavy Duty Vehicle traffic, respectively, was reported (Eleftheriadis et al., 2021), to be compared with a -73% decrease in driving route requests. However, changes in gasoline consumption are everywhere less than the variations in Apple® driving route requests (range 38% –88%, average 59%) as shown in Table S5.

For the set of cities where urban measurement sites were located, the Apple® mobility data show that driving route requests dropped by -31 % (Helsinki) to -90 % (Seville) between periods A and D, and increased again by +40 % (Helsinki) to +270 % (Paris) between periods D and P (Figure 2). The data recorded in the areas surrounding the regional background sites and/or the urban sites show similar variations, except for the Vysocina region (central Czech Republic) where driving route request numbers (-27 %) fell much less than in Prague (-60 %), and reached again their pre-lockdown value (period A) when lockdown measures were relaxed (period P).

According to monthly mean data available from CYSTAT, the road transport index in Cyprus decreased by -21 % in March 2020, by further -35 % in April 2020, and increased again by +18 % in May 2020 (Figure S2), in line with the mobility data collected for the other sites.

These data suggest that at least passenger car traffic strongly decreased as lockdown measures were implemented (period D) in all countries considered in this study, and particularly in Belgium, France, Italy, Spain, Greece and Cyprus. They also suggest that the road traffic intensity was largely greater by the end of May 2020 (period P) than during lockdown periods (period D) at all sites, but without reaching the intensities observed before (period A) at sites in Belgium, France, Italy, Spain, Greece and possibly Cyprus. However, 2020 monthly automotive fuel consumption data suggest that light and heavy-duty vehicle traffic (diesel) was much less reduced than private car (diesel + gasoline) traffic during the first lockdown period across Europe (Section 2.1, Table S5).

3.2 Impact of lockdown measures on PM mass concentrations

235   It is reminded here again that only sites for which the correlation between modelled and measured PM mass concentrations was satisfactory (positive slope, $R^2 \geq 0.5$) across the February – May 2019 period were considered (Table S4).

Figure 3 shows the mean observed / expected $PM_{2.5}$ and PM_{10} mass concentration ratios (Eq. 3) at urban sites during the 3 time periods defined as before (A), during (D) and after (P) the lockdowns. The differences between
240   these 3 values represent our estimates of the lockdown measures' impacts on pollutant atmospheric concentrations. As already observed across Europe (EEA, 2020; Shi et al., 2021) and the USA (Bekbulat et al., 2021), there was no systematic response of PM mass concentrations to the lockdown measures at urban sites. Indeed, the implementation of lockdown measures in March led to statistically significant decreases in $PM_{2.5}$ concentrations in Oslo, Rotterdam, and Barcelona (3 among 10 sites), and to a significant decrease in PM_{10}
245   concentration in Barcelona and Seville (2 out of 12 sites) only. On average (Table 2), the implementation of the lockdown measures resulted in minor increases in $PM_{2.5}$ and PM_{10} mass concentration of +1 ± 42 % and +5 ± 33 %, respectively. In contrast, the relaxation of lockdown measures in May led to statistically significant increases in $PM_{2.5}$ concentrations in Helsinki, Rotterdam, Brussels, Prague, Bern and Barcelona (6 out of 10 sites), and to a significant increase in PM_{10} concentrations in Rotterdam, Lille, Prague, Paris, Milan, Barcelona, and Nicosia (7
250   out of 12 sites). On average, the relaxation of the lockdown measures led to $PM_{2.5}$ and PM_{10} concentration increases of +26 ± 21 % and +26 ± 24 %, respectively. Where significant, lockdown measures had very similar impacts on $PM_{2.5}$ and PM_{10} concentrations. Lockdown impacts on PM concentrations in cities did generally not well reflect the variations in road traffic intensity expected from the driving road request data (Figure 2) as illustrated by Figure S3.

255   Advection from surrounding areas have been shown to contribute to PM concentrations in European cities (e.g. Kiesewetter et al., 2015; Thunis et al., 2018; Pommier et al., 2020). For example, modelling indicates that the contribution of sources outside the greater city contribute from 35 % (Paris, Athens) to 94 % (Nicosia) to $PM_{2.5}$ urban background concentrations in the cities considered here (Thunis et al., 2017).

Figure 4 shows the mean observed / expected $PM_{2.5}$ and PM_{10} mass concentration ratios (Eq. 3) during the 3 time
260   periods "before" (A), "during" (D) and "after" (P) the lockdowns at regional background sites in the regions of the cities mentioned above. The implementation of lockdown measures led to statistically significant decreases in $PM_{2.5}$ concentration in BIR (NO), and in PM10 concentrations in BIR and MEL (DE) only (3 out of 16 entries), while their relaxation resulted in significant increases in $PM_{2.5}$ concentrations in BIR, CBW (NL), MEL, KOS (CZ), SIR (FR), and in PM_{10} concentrations in BIR, CBW, MEL, SIR, PAY (CH), and IPR (IT), i.e., 11 out of 16
265   entries. At regional background sites, lockdown implementations resulted on average, in +2 ± 39 % and +15 ± 42 % increases in $PM_{2.5}$ and PM_{10} mass concentrations, respectively. Their relaxation resulted in further +38 ± 43 % and +28 ± 10 % increases in $PM_{2.5}$ and PM_{10} concentrations, respectively. Comparing PM data with the driving route request data in Figure 2 (bottom) suggests no significant impact of private car traffic intensity on regional background PM levels (Figure S4).

270   There is generally no correspondence between significant lockdown impacts on PM concentrations at twin sites (urban and regional background sites located in the same area), except for Oslo-BIR (PM decrease from A to D), and Rotterdam-CBW, Prague-KOS, Paris-SIR, and Milan-IPR (PM increase from D to P).

Due to the multiplicity of PM primary and secondary sources, further atmospheric variables such as gaseous pollutant concentrations and PM intrinsic characteristics shall be examined to investigate the lack of dramatic
275   drops in PM mass concentrations resulting from the reduction in private car traffic when lockdown measures were implemented at the sites considered in this study.

3.3 Impact of lockdown measures on NO_2 concentrations

Road traffic is the major source of NO_x (nitrogen oxides) in Europe (EEA, 2020). For the 15 cities considered in this study, the contribution of road traffic to annual NO_x emissions ranges from 35 % in Rotterdam to 95 % in
280   Athens (Degraeuwe et al., 2019). Road-traffic intensity variations are therefore expected to significantly affect NO_2 concentrations. Diesel engines are by far the largest contributors to road traffic NO_x emissions in most countries across Europe, a noticeable exception being Greece (2016 data). However, for all 13 countries considered, the passenger car fleet emits the largest share of NO_x (60 – 90 %), far ahead that of the light duty plus heavy duty vehicle fleet. Since mobility restrictions presumably affected mostly passenger cars (Section 3.1),

285   dramatic variations in driving route requests (as a proxy for vehicle kilometres) are expected to result in significant changes in road traffic NO_x emissions.

Lockdown measure implementations led to statistically significant decreases in NO_2 concentrations in Helsinki, Copenhagen, Rotterdam, Brussels, Lille, Paris, Bern, Milan, and Barcelona, i.e., in 9 among 13 cities. At sites where no significant reduction in NO_2 concentrations occurred, there was no significant decreases in nitrogen

290   oxide (NO) concentrations either (Figure S5), indicating no substantial abatement of NO_x emissions. On average, the implementation of lockdown measures resulted in NO_2 concentration decreasing by -29 ± 17 %. Lockdown measure relaxations led to significant rebounds in NO_2 concentrations in Copenhagen, Brussels, Lille, Prague, Paris, Milan, and Seville (7 among 13 cities). The mean increase in NO_2 concentration resulting from the lockdown termination was +31 ± 30 %. Although the impact of the lockdown measures was more systematic for

295   NO_2 than for PM concentrations (Figure S6), there is no significant correlation between the impact on NO_2 concentration and the reduction in driving route requests from periods A to D, and only a marginally significant correlation between the impact on NO_2 concentration and the increase in driving route requests from periods D to P (Figure S3).

Lockdown measures also resulted in significant decreases in NO_2 concentrations at 7 of the 12 regional

300   background sites (HYY, FI; CBW, NL; SIR, FR; PAY, CH; IPR, IT; CYP, CY). Their relaxation led to significant increases in NO_2 at 3 sites only, namely CBW (NL), MEL (DE), and SIR (FR). On average, the implementation and relaxation of lockdown measures resulted in a -17 ± 24 % decrease and +27 ± 50 % increase in NO_2 concentration at regional background sites, respectively. There is no statistically significant correlation (95 % confidence level) between the lockdown impact on NO_2 concentrations and the changes in route request data from

305   periods A to D and D to P at the regional background sites (Figure S4).

Figure 5 shows that there is generally no matching in NO_2 ratio variations from periods A to D, and from periods D to P, between urban sites and regional background sites in surrounding areas (with a few exceptions including Paris-SIR and Bern-PAY), which suggests that NO_2 concentrations at urban and regional background sites are controlled by different sources and /or atmospheric processes.

310   The lack of systematic correlation between the variations in the Apple® driving route request index and the changes in NO_2 concentrations due to the lockdown implementation and relaxation measures suggests that the linkage between passenger car traffic and NO_x emissions was not that straightforward under such circumstances. However, NO_2 being an important precursor of secondary PM, and the vehicles that emit most NO_x being also those which emit most primary PM, the lack of dramatic impact of lockdowns on PM concentrations compared

315   to their clear effect on NO_2 concentrations at many sites emphasises the variety of PM sources and the complexity of secondary formation processes.

3.4 Impact of lockdown measures on O_3 concentrations

Implementations of lockdown measures induced statistically significant increases in O_3 concentrations in Brussels, Lille, Paris, Barcelona, and Nicosia, i.e., in 5 cities out of 12, Milan being on the edge (Figure 6, top).

320   There were no cities where lockdown measures led to a significant decrease in O_3. This is consistent with photochemical O_3 production not being limited by the availability of NO_x in urban areas, and with a reduction of O_3 titration by NO as resulting from an abatement in NO_x emissions during the lockdown periods. On average, the implementation of the lockdown measures resulted in an increase of +11 ± 23 % in O_3 concentration in cities. Also at the regional background sites BIR (NO), KOS (CZ), SIR (FR), IPR (IT) and ARN (ES), the effect of the

325   lockdown measures was a significant increase in O_3 concentrations, and at no sites was a significant decrease in O_3 detected. This is again consistent with an excess of NO_x in O_3 photochemical formation at those sites, at least during this period of the year (February – April). The significant increase in O_3 after the lockdown measure relaxation (period P) in BIR (NO), and ARN (ES) could be explained by a shift in the O_3 photochemical production to the "NO_x limited" regime at these regional background sites, resulting from increased emissions of biogenic

330   volatile organic species in May. On average, the impact of the lockdown measures implementation and relaxation on O_3 concentration at regional background sites was estimated to +17 ± 24 % and +4 ± 5 %, respectively.

Increased O_3 concentrations reflect an increase in the oxidizing capacity of the atmosphere. The increased oxidizing capacity of the atmosphere was invoked to explain the lack of systematic decrease in PM concentrations resulting from the lockdown measures (e.g. Kroll et al., 2020): the expected decrease in PM primary emissions

335   would be compensated (or even over-compensated) by an increased production of secondary aerosol resulting from a faster oxidation of PM gaseous precursors to condensable material. Actually, increased aerosol surface

area and Aitken mode particle growth rates were observed for the lockdown period in Athens (Eleftheriadis et al., 2021), together with increases in O_3 and $PM_{2.5}$ concentrations. This hypothesis is to some extent also supported by recent modelling works (Clappier et al., 2021) suggesting that in the areas surrounding Rotterdam, Bern, Milan, and Barcelona, reduction in NO_x emissions would lead to enhanced secondary PM formation resulting from the increased oxidizing capacity of the atmosphere. However, the magnitude of this phenomenon during the 2020 lockdown could only be assessed on the basis of detailed PM chemical composition data (including not only sulfate and nitrate, but also secondary organics), which are not available at the sites located in these areas considered under our study.

In the following sections, other possibilities will be examined by making use of specific aerosol properties, which are not part of the air pollution regulated metrics.

3.5 Impact of the lockdown measures on aerosol intrinsic characteristics

A reason why lockdown impacts on PM mass concentrations were smaller than expected could be the compensation of the decrease in road traffic emissions by the increase in domestic heating emissions, resulting from people "staying-at-home" (Altuwayjiri, et al., 2021). Since wood (or wood pellets) is one of the fuels used for domestic heating, any decrease in road traffic compared to domestic heating emissions would result in an increase of the AÅE. We also deemed it important to assess how clear was the lockdown effects on primary particle emissions from vehicle engines. This is why the contribution of small particles (D_p<70 nm) to the total particle number (N_{small} / N_{tot}) was examined. The measurement data needed to calculate these intensive variables were not available for all the 28 sites considered in this study (see Table S3). Therefore, data from urban and regional background sites are not split in separate figures for these two variables.

3.5.1 Particle light absorption spectral dependence

A statistically significant impact of the lockdown measure implementation and relaxation on the particle light absorption spectral dependence was detected in Lille (FR), Athens (GR) and ARN only (Figure 7). At both urban sites, 2020 AÅE values were very similar to the 2017 -2019 averages for periods A and P, and significantly greater during the lockdown period (D). AÅE values also significantly increased as lockdown measures were implemented in Oslo (NO) and SIR (FR), while AÅE values significantly decreased as lockdown measures were relaxed in IPR (IT). No significant change in 2020 AÅE values (as compared with 2017 - 2019) could be observed for the lockdown period (D) in BIR (NO), Brussels (BE), KOS (CZ), Bern (CH), PAY (CH), and MSY (ES). On average (all site types), the AÅE increased by +3 ± 6 % and decreased by -8 ± 28 % as lockdown measures were implemented and relaxed. In short, the expected increase in AÅE resulting from a decrease in particle emissions from traffic and a stagnation or increase in particulate emissions from wood burning during the lockdown period was not systematically observed across the sites considered in this study. Therefore, increased emissions from domestic heating during the lockdown can have contributed to maintain unexpectedly high PM mass concentrations in certain places across Europe, but this phenomenon was apparently not relevant in many areas.

3.5.2 Particle number size distribution

At 3 of the 5 urban sites for which data were available (Leipzig, Athens, and Granada), the implementation of the lockdown measures in 2020 coincided with a statistically significant decrease in the N_{small} / N_{tot} ratio as compared to the same time periods in 2017 – 2019 (Figure 8). A significant increase in this ratio occurred as lockdown measures were relaxed at only 2 amongst the 6 urban sites with relevant data (Copenhagen and Barcelona). On average, the implementation and relaxation of lockdown measures corresponded to a decrease by -7 ± 5 % and an increase by +6 ± 2 %, respectively, in the N_{small} / N_{tot} ratio.

These observations suggest that the decrease in traffic resulting from the implementation of the lockdown measures led on average to a significant but moderate decrease in the number concentration of primary ultrafine particles (which dominate the 15 – 70 nm size range in urban environments). The lack of complete return to usual PNSDs after the lockdown period ended can be explained by only partial recovery in human mobility in Athens (GR) and Granada (ES), but not in Leipzig (DE) where mobility almost completely (95 %) recovered.

During the lockdown period (D), statistically significant changes in the contribution of small particles to the whole PNSD (N_{small} / N_{tot}) were also detected at 4 out of 6 regional background sites, i.e. BIR (NO), RIS (DK), MEL (DE) and IPR (IT). Variations in RIS and MEL reflected quite well the variations in the nearby cities of Copenhagen and Leipzig. Clear decreases and increases in N_{small} / N_{tot} corresponding to the lockdown measures

implementation and relaxation, respectively, can be noticed at both BIR (NO) and IPR (IT). The variations observed in IPR can easily be related to the variations in the driving route request index for the densely populated and traffic impacted Lombardy region. In contrast, it is surprising to observe such significant changes in the PNSD in BIR, located in a region (Agder) where the driving mobility index remained relatively high, even during the lockdown period. Lockdown measures also had a huge impact on PM mass concentration in BIR (Figure 3), but providing a specific explanation for the case of BIR is beyond the scope of this study. On average, the implementation and relaxation of lockdown measures coincided with a decrease by -9 ± 13 % and an increase by +11 ± 12 %, respectively, in the N_{small} / N_{tot} ratio at regional background sites.

In short, except for the two sites located in Finland, the lockdown periods coincided with unusual low shares of small particles (N_{small} / N_{tot}) at all sites, although differences were not all statistically significant. This suggests that the lockdown measures did have an impact on primary particle emissions. However, considering the huge changes in the driving route request index for a vast majority of sites in this study, the impact on PNSD was not quite dramatic. This suggests that private cars do not significantly contribute to the overall emission of 15-70 nm particles at the sites we studied, or that the decrease in this specific source was compensated by increases in other sources (including nucleation and growth of new particles) during the lockdown periods.

4 Conclusions

Specific impacts on air pollution of the implementation and relaxation of lockdown measures to prevent the spread of COVID-19 were determined by comparing observations with expected data for the period 17 February – 31 May 2020 (Table 2).

Driving direction request data suggest that the reduction in car passenger traffic resulting from the lockdown measures was much more pronounced in the southern Europe than in northern Europe. Regardless the variations in these human mobility indicators, we did not observe statistically significant decreases in $PM_{2.5}$ and PM_{10} mass concentrations at most of the European urban sites considered in our analysis. Consequently, the implementation of lockdown measures in March 2020 did not lead on average to a decrease in $PM_{2.5}$ and /or PM_{10} mass concentrations across these sites. In contrast, the relaxation of the lockdown measures in May 2020 led to an increase of $PM_{2.5}$ and /or PM_{10} concentrations at more than half of the cities studied, resulting in a mean increase of +26 % in both $PM_{2.5}$ and PM_{10} concentrations. At regional background sites, the implementation of the lockdown measures yielded a significant impact at an even more limited number of sites, whereas their relaxation resulted in $PM_{2.5}$ and/or PM_{10} mass concentration increases at most of them. The asymmetrical response of PM mass concentrations to the implementation and relaxation of lockdown measures suggests a relationship more complex than expected between road traffic intensity and PM mass concentrations. By looking at a range of other atmospheric variables, we gained more insights into this phenomenon.

Regarding key gaseous pollutants, NO_2 concentrations significantly decreased at 3/5 of the urban sites due to the implementation of lockdown measures, and significantly re-increased at 3/10 of them due to their relaxation. On average, the implementation and relaxation of lockdowns resulted in a notable -29 % decrease and in a +31 % rebound in NO_2 concentration, respectively. These figures suggest that mobility restrictions did translate into decreases in road traffic NO_x emissions. However, the extent of the changes in NO_2 concentrations did not correlate well with the changes in human mobility. This disparity could be attributed to the fact that driving route request indices differently reflected the number of km driven in various countries, and by different proportion of vehicles complying with the various EURO emission standards across Europe.

The implementation of lockdown measures also altered the oxidizing capacity of the atmosphere, potentially resulting in the formation of a larger amount of secondary aerosols during lockdown periods, despite lower levels of gaseous precursors. Specifically, our study revealed a significant increase in O_3 concentrations (an indicator of the oxidizing capacity of the atmosphere) due to the lockdown implementation at 1/2 of the urban and regional background sites. The production of secondary particulate matter could have been boosted at these sites. Modelling work by Clappier et al. (2021) demonstrated that decreases in NO_x emissions would result in increased secondary PM concentrations in some parts of Europe . Nevertheless, additional data pertaining to the aerosol chemical composition would be needed to ascertain whether this process exerted a substantial impact on PM mass concentrations as lockdown measures were implemented at the studied sites.

Possible changes in some intrinsic aerosol properties (such as the light absorption spectrum and the particle size distribution shape) were also assessed in this work. The occurrence of significantly higher AÅE values during the

lockdown periods at a few sites in Norway, France, Italy, Greece and Spain indicates a relatively larger contribution of black carbon from wood burning as compared to fossil fuel burning during these periods. Therefore, the decrease in PM concentrations associated with traffic-related sources could have been partially offset to activities by an increase in PM concentrations related to domestic heating at these sites. However, this phenomenon was apparently not generalised throughout Europe.

Regarding PNSD, a statistically significant lockdown effect was observed at most of the studied sites. On average, moderate -7 % and -9 % decreases were observed in the contribution of small particles to the total particle number concentration across urban and regional background sites, respectively. These figures indicate that the implementation of lockdown measures resulted in a decrease in primary particle emissions (predominantly in the 15 – 70 nm range) compared to the production of secondary particles (mainly in the range 100 – a few hundreds of nm). Consequently, it is suggested that measures leading to a reduction in passenger car traffic (as lockdown measures did) would likely have a larger impact on particle number concentrations (which are strongly dependent on the abundance of small particles) than on PM mass concentrations (which are more sensitive to the number of particles in the range 70 – several hundreds of nm) in urban areas.

Our results on PM_{10} and $PM_{2.5}$ align with previous studies that similarly reported limited impacts of lockdowns on PM mass concentrations over Europe and the USA (Archer et al., 2020; Bekbulat et al., 2021; Shi et al., 2021; Querol et al., 2021). However, they contrast with other findings, that indicated substantial reductions in PM mass concentrations in several big European and American cities due to the COVID-19 lockdown measures (Chauhan and Singh, 2020; Beloconi et al., 2021; Jiang et al., 2021). Several factors could help explain these contrasting observations: (i) the effectiveness of lockdown measures in reducing PM mass concentrations can vary across different regions due to variations in factors such as population density, variability of the pollution sources such as industrial activities and transportation patterns, and meteorological conditions; (ii) the level of stringency, duration and adherence to lockdown measures can vary between different countries or even within different regions of the same country; (iii) the response of different PM chemical constituents to lockdown measures can vary, leading to varying observations across studies when only whole PM_{10} or $PM_{2.5}$ mass concentrations are considered; (iv) the existing pollution levels before the implementation of lockdown measures can influence the magnitude of changes observed during the lockdown period. If the baseline pollution levels were already low, the impact of lockdown measures may be less detectable compared to areas with higher initial pollution levels.

Overall, this comprehensive study encompassing 28 European sites enhances our understanding of the human of human mobility restriction on particulate air pollution, leveraging the unique circumstances of COVID-19 lockdowns. In particular, we highlighted the complexity of PM mass concentration responses to the COVID lockdown measures implemented throughout Europe, which arise from a combination of several factors. These include uneven levels of stringency in the across different European countries, evidenced compensation between road traffic and domestic heating emissions at some sites, and the potential for heightened formation of secondary PM at other sites. Quantitatively assessing the distinct contributions of these phenomena across Europe remains an important task for future research that goes beyond the scope of this study. Nevertheless, the "experiment" presented by the COVID-19 lockdowns suggests that the on-going decrease in exhaust emissions by the passenger car fleet might yield quite contrasting impacts on air quality in European cities.

Disclaimer

The information and views set out are those of the authors and do not necessarily reflect the official opinion of the European Commission.

Competing interests

One of the co-authors is a member of the editorial board of Atmospheric Chemistry and Physics. The peer-review process was guided by an independent editor, and the authors have also no other competing interests to declare.

Author contributions

Conceptualization and methodology: JPP and EP. Formal analysis: JPP. Investigation: JPP, AM, CH, JS, MP, JO, SM, KW, MM, LP, DvP, AM, CN, CR, NP, SC, MS, JAA, TP, KL, JN, VR, JFdB, AC, OF, JEP, VG, MIG, SV, ED, HDvdG, KEY, WA. Original draft preparation: JPP. Review and editing: EP, AM, CH, MP, JO, SM, AW, LP, HH, AM, AA, NP, SC, MS, JAA, KL, JN, VR, JFdB, AC, KE, HDvdG, WA.

Data availability

Observation data from ACTRIS observatories are available at actris.nilu.no and ebas.nilu.no. Observation data from urban sites are available from local Air Quality Monitoring Networks and from www.eea.europa.eu/data-and-maps/data/aqereporting-9. Model forecasts for all sites are available at ads.atmosphere.copernicus.eu/cdsapp#!/dataset/cams-europe-air-quality-forecasts?tab=form.

Acknowledgements

The research presented here relied on the data and products made available in open access, by the Copernicus Atmosphere Monitoring Service (CAMS) of the Copernicus Programme of the European Union, and in particular the CAMS Policy Service, //policy.atmosphere.copernicus.eu/.

PNSD and particle light absorption data were provided by the ACTRIS Data Centre developed under the European Union's Horizon 2020 research and innovation programme under grant agreement No 654109 (ACTRIS-2). Data quality assurance has been supported by the ACTRIS-IMP project of the European Commission under grant agreement No 871115.

The Belgian Interregional Environment Agency (Ircel-Celine) is acknowledged for the provision of PM_{10}, $PM_{2.5}$, NO, NO_2 and O_3 data from Brussels.

Czech Hydrometeorological Institute provided air quality monitoring data from Prague (Libus). Conditions of data utilization (in Czech): www.chmi.cz/files/portal/docs/uoco/historicka_data/OpenIsko_data.

Data from Leipzig-West was kindly provided by the Saxon State Office for the Environment, Agriculture and Geology (LfULG).

IMT Nord Europe acknowledges financial support from the Labex CaPPA project, which is funded by the French National Research Agency (ANR) through the PIA (Programme d'Investissement d'Avenir) under contract ANR-11-LABX-0005-01, and the CLIMIBIO project, both financed by the Regional Council "Hauts-de-France" and the European Regional Development Fund (ERDF). IMT Nord Europe participated in the COST COLOSSAL Action CA16109. The ATOLL site (Lille) is one of the French ACTRIS National Facilities and contributes to the CARA program of the LCSQA funded by the French Ministry of Environment.

Airparif, the agency for air quality monitoring in the Ile-de France region, kindly provided open access to air quality data.

ARPA Lombardia kindly provided air quality data from Milan.

The Rotterdam EPA (DCMR) kindly provided air quality measurements in Rotterdam.

References

Altuwayjiri, A., Soleimanian, E., Moroni, S., Palomba, P., Borgini, A., De Marco, C., Ruprecht, A.A., Sioutas, C.: The impact of stay-home policies during Coronavirus-19 pandemic on the chemical and toxicological characteristics of ambient PM2.5 in the metropolitan area of Milan, Italy, Sci. Total Environ. 758, https://doi.org/10.1016/j. scitotenv.2020.143582, 2021.

Archer, C.L., Cervone, G., Golbazi, M., Al Fahel, N., Hultquist, C.: Changes in air quality and human mobility in the USA during the COVID-19 pandemic, *Bull. of Atmos. Sci.& Technol.* **1**, 491–514, https://doi.org/10.1007/s42865-020-00019-0, 2020.

Barré, J., Petetin, H., Colette, A., Guevara, M., Peuch, V.-H., Rouil, L., Engelen, R., Inness, A., Flemming, J., Pérez García-Pando, C., Bowdalo, D., Meleux, F., Geels, C., Christensen, J. H., Gauss, M., Benedictow, A., Tsyro, S., Friese, E., Struzewska, J., Kaminski, J. W., Douros, J., Timmermans, R., Robertson, L., Adani, M., Jorba, O., Joly, M., and Kouznetsov, R.: Estimating lockdown-induced European NO_2 changes using satellite and surface observations and air quality models, Atmos. Chem. Phys., 21, 7373–7394, https://doi.org/10.5194/acp-21-7373-2021, 2021.

Bekbulat, B., Apte, J. S., Millet, D. B., Robinson, A. L., Wells, K. C., Presto, A. A., and Marshall, J. D.: Changes in criteria air pollution levels in the US before, during, and after Covid-19 stay-at-home orders: Evidence from regulatory monitors, Sci. Total Environ., 769, 144693, doi.org/10.1016/j.scitotenv.2020.144693, 2021.

Beloconi, A., Probst-Hensch, N. M., and Vounatsou, P.: Spatio-temporal modelling of changes in air pollution exposure associated to the COVID-19 lockdown measures across Europe, Sci. Total Environ., 787, 147607, doi.org/10.1016/j.scitotenv.2021.147607, 2021.

Cerqua, A., Di Stefano, R.: When did coronavirus arrive in Europe? Stat Methods Appl 31, 181–195, doi.org/10.1007/s10260-021-00568-4, 2022.

Chauhan, A. and Singh, R. P.: Decline in $PM_{2.5}$ concentrations over major cities around the world associated with COVID-19, Environ. Res., 187, 109634, https://doi.org/10.1016/j.envres.2020.109634, 2020.

Clappier, A., Thunis, P., Beekmann, M., Putaud, J.P., Demeij, A.: Impact of SOx, NOx and NH_3 emission reductions on $PM_{2.5}$ concentrations across Europe: Hints for future measure development, Environment International, 156, doi.org/10.1016/j.envint.2021.106699, 2021.

Copernicus, atmosphere.copernicus.eu/flawed-estimates-effects-lockdown-measures-air-quality-derived-satellite-observations, 2020.

Degraeuwe, B., Pisoni, E., Peduzzi, E., De Meij, A., Monforti-Ferrario, F., Bodis, K., Mascherpa, A., Astorga-Llorens, M., Thunis, P. and Vignati, E.: Urban NO_2 Atlas, EUR 29943 EN, Publications Office of the European Union, Luxembourg, ISBN 978-92-76-10387-5, doi:10.2760/538816, JRC118193, 2019.

Denier van der Gon, H. A. C., Bergström, R., Fountoukis, C., Johansson, C., Pandis, S. N., Simpson, D., and Visschedijk, A. J. H.: Particulate emissions from residential wood combustion in Europe – revised estimates and an evaluation, Atmos. Chem. Phys., 15, 6503–6519, https://doi.org/10.5194/acp-15-6503-2015, 2015.

EEA, European Environment Agency: Air quality in Europe — 2020 report, EEA Report No 11/2020, available at: https://www.eea.europa.eu/publications/air-quality-in-europe-2020-report (last access: 24 March 2023), 2020.

Eleftheriadis, K., Gini, M.I., Diapouli, E., Vratolis, S., Vasilatou, V.,Fetfatzis, P., Manousakas, M. I.: Aerosol microphysics and chemistry reveal the COVID19 lockdown impact on urban air quality, Sci Rep 11, 14477, https://doi.org/10.1038/s41598-021-93650-6, 2021.

Galmarini, S., Kioutsioukis, I., Solazzo, E., Alyuz, U., Balzarini, A., Bellasio, R., Benedictow, A. M. K., Bianconi, R., Bieser, J., Brandt, J., Christensen, J. H., Colette, A., Curci, G., Davila, Y., Dong, X., Flemming, J., Francis, X., Fraser, A., Fu, J., Henze, D. K., Hogrefe, C., Im, U., Garcia Vivanco, M., Jiménez-Guerrero, P., Jonson, J. E.,

Garbariene, I.; Dudoitis, V.; ̇Ulevicius, V.; Plauškaite-Šukiene, K.; Kilikevicius, A.; Matijošius, J.; Rimkus, A.; Kilikeviciene, K.; Vainorius, D.; Maknickas, A.; Borodinas, S and Bycenkiene, S.: Application of Acoustic Agglomeration Technology to Improve the Removal of Submicron Particles from Vehicle Exhaust. Symmetry, 13, 1200. doi.org/10.3390/sym13071200, 2021.

Giechaskiel, B.: Particle Number Emissions of a Diesel Vehicle during and between Regeneration Events. Catalysts, 10, 587, doi.org/10.3390/catal10050587, 2020.

Goldberg, D. L., Anenberg, S. C., Griffin, D., McLinden, C. A., Lu, Z., and Streets, D. G.: Disentangling the Impact of the COVID-19 Lockdowns on Urban NO_2 from Natural Variability, Geophys. Res. Lett., 47, e2020GL089269, https://doi.org/10.1029/2020GL089269, 2020.

Grange, S. K., Lee, J. D., Drysdale, W. S., Lewis, A. C., Hueglin, C., Emmenegger, L., and Carslaw, D. C.: COVID-19 lockdowns highlight a risk of increasing ozone pollution in European urban areas, Atmos. Chem. Phys., 21, 4169–4185, https://doi.org/10.5194/acp-21-4169-2021, 2021.

Hammer, M.S., van Donkelaar, A., Martin, R.V., McDuffie, E.E., Lyapustin, A., Sayer, A.M., Hsu, N.C., Levy, R.C., Garay, M.J., Kalashnikova, O.V., Kahn, R.A.: Effects of COVID-19 lockdowns on fine particulate matter concentrations, *Sci. Adv.*, 7, 26, eabg7670, DOI:10.1126/sciadv.abg7670, 2021.

Helin, A., Virkkula, A., Backman, J., Pirjola, L., Sippula, O., Aakko-Saksa, P., et al.: Variation of absorption Ångström exponent in aerosols from different emission sources. Journal of Geophysical Research: Atmospheres, 126(10), e2020JD034094, https://doi.org/10.1029/2020JD034094, 2021.

Hueglin, C., Gaegauf, C., Künzel, S. and Burtscher, H.: Characterization of Wood Combustion Particles: Morphology, Mobility, and Photoelectric Activity, Environmental Science & Technology 31 (12), 3439-3447, DOI: 10.1021/es970139i, 1997.

IEA, International Energy Agency, Global Energy Review 2020: The impacts of the Covid-19 crisis on global energy demand and CO_2 emissions, www.iea.org/reports/global-energy-review-2020, 2020.

Jiang, Z., Shi, H., Zhao, B., Gu, Y., Zhu, Y., Miyazaki, K., Lu, X., Zhang, Y., Bowman, K. W., Sekiya, T., and Liou, K.-N.: Modeling the impact of COVID-19 on air quality in southern California: implications for future control policies, Atmos. Chem. Phys., 21, 8693–8708, https://doi.org/10.5194/acp-21-8693-2021, 2021.

585   Kiesewetter, G., Borken-Kleefeld, J., Schöpp, W., Heyes, C., Thunis, P., Bessagnet, B., Terrenoire, E., Fagerli, H., Nyiri, A., and Amann, M.: Modelling street level PM_{10} concentrations across Europe: source apportionment and possible futures, Atmos. Chem. Phys., 15, 1539–1553, doi.org/10.5194/acp-15-1539-2015, 2015.

Kroll, J.H., Heald, C.L., Cappa, C.D, Farmer, D.K., Fry, J.L., Murphy, G.L., Steiner, A.L.: The complex chemical effects of COVID-19 shutdowns on air quality. *Nat. Chem.* 12, 777–779, https://doi.org/10.1038/s41557-020-0535-z, 2020.

590

Kuenen, J., Dellaert, S., Visschedijk, A., Jalkanen, J.-P., Super, I., and Denier van der Gon, H.: CAMS-REG-v4: a state-of-the-art high-resolution European emission inventory for air quality modelling, Earth Syst. Sci. Data, 14, 491–515, https://doi.org/10.5194/essd-14-491-2022, 2022.

Le, T., Wang, Y., Liu, L., Yang, J., Yung, Y.L., Li, G., Seinfeld, J.H.: Unexpected air pollution with marked 595   emission reductions during the COVID-19 outbreak in China, Science **369**, 702–706, 2020.

Marecal, V., Peuch, V.-H., Andersson, C., Andersson, S., Arteta, J., Beekmann, M., Benedictow, A., Bergström, R., Bessagnet, B., Cansado, A., Chéroux, F., Colette, A., Coman, A., Curier, L., Denier van der Gon, H., Drouin, A., Elbern, H., Emili, E., Engelen, R., Ung, A.: A regional air quality forecasting system over Europe: the MACC-II daily ensemble production. Geoscientific Model Development, 8, 2777–2813, doi:10.5194/gmd-8-2777-2015, 600   2015.

Meppelink, J., van Langen, J., Siebes, A., Spruit, M.; Visvizi, A.: .Beware Thy Bias: Scaling Mobile Phone Data to Measure Traffic Intensities, Sustainability, 12(9), 3631, //doi.org/10.3390/su12093631, 2020.

Ou, S., He, X., Ji, W., Chen, W., Sui, L., Gan, Y., Lu, Z., Lin, Z., Deng, S., Przesmitzki, S., Bouchard, J.: Machine learning model to project the impact of COVID-19 on US motor gasoline demand, Nature Energy, 5(9), 666–673, 605   //doi.org/10.1038/s41560-020-0662-1, 2020.

Petetin, H., Bowdalo, D., Soret, A., Guevara, M., Jorba, O., Serradell, K., and Pérez García-Pando, C.: Meteorology-normalized impact of the COVID-19 lockdown upon NO_2 pollution in Spain, Atmos. Chem. Phys., 20, 11119–11141, //doi.org/10.5194/acp-20-11119-2020, 2020.

Petit, J.-E., Dupont, J.-C., Favez, O., Gros, V., Zhang, Y., Sciare, J., Simon, L., Truong, F., Bonnaire, N., Amodeo, 610   T., Vautard, R., and Haeffelin, M.: Response of atmospheric composition to COVID-19 lockdown measures during spring in the Paris region (France), Atmos. Chem. Phys., 21, 17167–17183, https://doi.org/10.5194/acp-21-17167-2021, 2021.

Pommier, M., Fagerli, H., Schulz, M., Valdebenito, A., Kranenburg, R., and Schaap, M.: Prediction of source contributions to urban background PM_{10} concentrations in European cities: a case study for an episode in 615   December 2016 using EMEP/MSC-W rv4.15 and LOTOS-EUROS v2.0 – Part 1: The country contributions, Geosci. Model Dev., 13, 1787–1807, doi.org/10.5194/gmd-13-1787-2020, 2020.

Putaud, J.-P., Pozzoli, L., Pisoni, E., Martins Dos Santos, S., Lagler, F., Lanzani, G., Dal Santo, U., and Colette, A.: Impacts of the COVID-19 lockdown on air pollution at regional and urban background sites in northern Italy, Atmos. Chem. Phys., 21, 7597–7609, https://doi.org/10.5194/acp-21-7597-2021, 2021.

620   Querol, X., Massagué, J., Alastuey, A., Moreno, T., Gangoiti, G., Mantilla, E., Duéguez, J.J., Escudero, M., Monfort, E., García-Pando, C.P., Oriol Jorba, H. P., Vázquez, V., de la Rosa Alberto Campos, J., Muñóz, M., Monge, S., Hervás, M., Javato, R., and Cornide, M. J.: Lessons from the COVID-19 air pollution decrease in Spain: Now what?, Sci. Total Environ., 779, 146380, https://doi.org/10.1016/j.scitotenv.2021.146380, 2021.

Riccio, A., Giunta, G., and Galmarini, S.: Seeking for the rational basis of the Median Model: the optimal 625   combination of multi-model ensemble results, Atmos. Chem. Phys., 7, 6085–6098, doi.org/10.5194/acp-7-6085-2007, 2007.

Schiermeier, Q.: Why pollution is plummeting in some cities—but not others. Nature. doi:10.1038/d41586-020-01049-6, 2020.

Shi, Z., Song, C., Liu, B., Lu, G., Xu, J., Van Vu, T., Elliott, R.J.R., Li, W., Bloss, W.J., Harrison, R.M: Abrupt but smaller than expected changes in surface air quality attributable to COVID-19 lockdowns, Sci. Adv. 7 (3), DOI:10.1126/sciadv.abd6696, 2021.

Thunis, P., Degraeuwe, B., Pisoni, E., Trombetti, M., Peduzzi, E., Belis, C.A., Wilson, J., Vignati, E.: Urban PM2.5 Atlas - Air Quality in European cities, EUR 28804 EN, Publications Office of the European Union, Luxembourg, ISBN 978-92-79-73876-0, doi:10.2760/336669, JRC108595, 2017.

Thunis, P., Degraeuwe, B., Pisoni, E., Trombetti, M., Peduzzi, E., Belis, C.A., Wilson, J., Clappier, A., Vignati, E.: PM2.5 source allocation in European cities: A SHERPA modelling study, Atmos. Environ., 187, 93-106, doi.org/10.1016/j.atmosenv.2018.05.062, 2018.

Venter, Z.S., Aunan, K., Chowdhury, S., Lelieveld, J.: COVID-19 lockdowns cause global air pollution declines. Proc. Natl. Acad. Sci. 117, 18984–18990, https://doi.org/10.1073/pnas.2006853117, 2020.

Yang, J., Wen, Y., Wang, Y., Zhang, S., Pinto, J. P., Pennington, E. A., Wang, Z., Wu, Y., Sander, S. P., Jiang, J. H., Hao, J., Yung, Y. L., and Seinfeld, J. H.: From COVID-19 to future electrification: Assessing traffic impacts on air quality by a machine-learning model, P. Natl. Acad. Sci. USA, 118, e2102705118, https://doi.org/10.1073/pnas.2102705118, 2021.

Figure 1. Location of the 28 sites across Europe (map background from ESA).
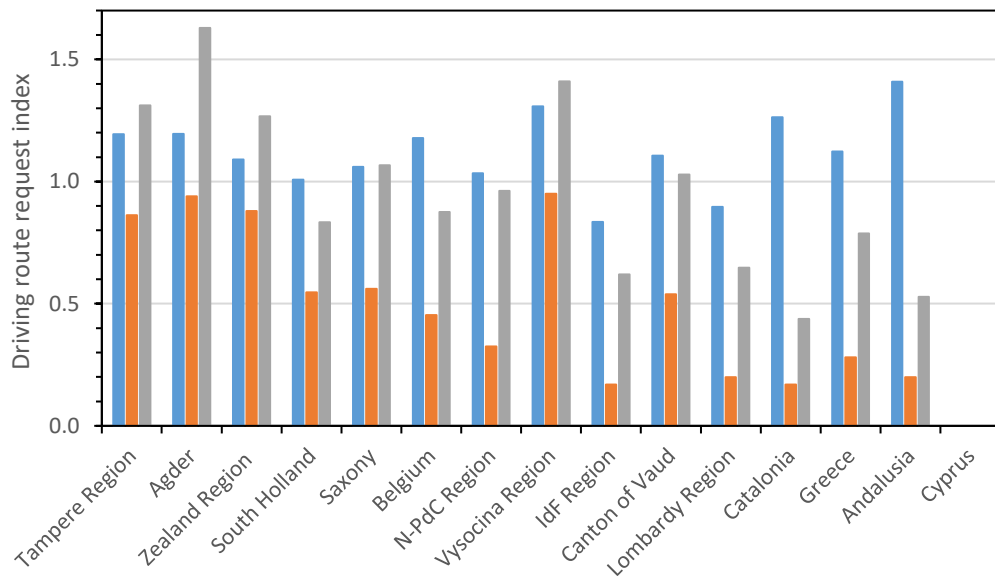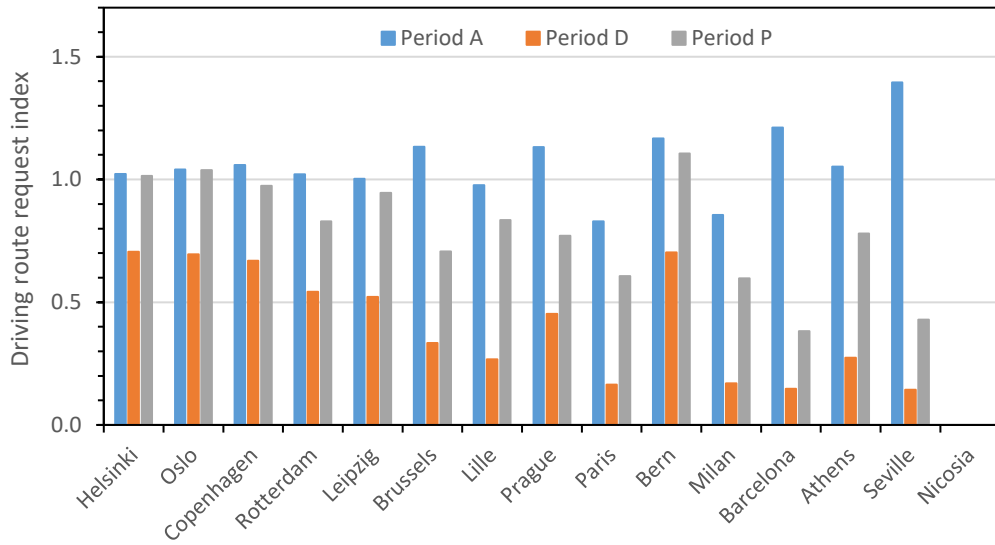
655

Figure 2. Driving route request indices during period A (17 February – 8 March), D (23 March– 3 May) and P (11 – 31 May) in cities where measurement sites were located (top), and in areas where regional background sites and/or urban sites were located (bottom). Apple® mobility indices are relative to data of 13 January 2020. Data from 11 and 12 May 2020 are missing. N-PdC and IdF stand for the French "Nord-Pas de Calais" and "Ile de France" regions, respectively. No data for Cyprus (see

660   Fig. S1).
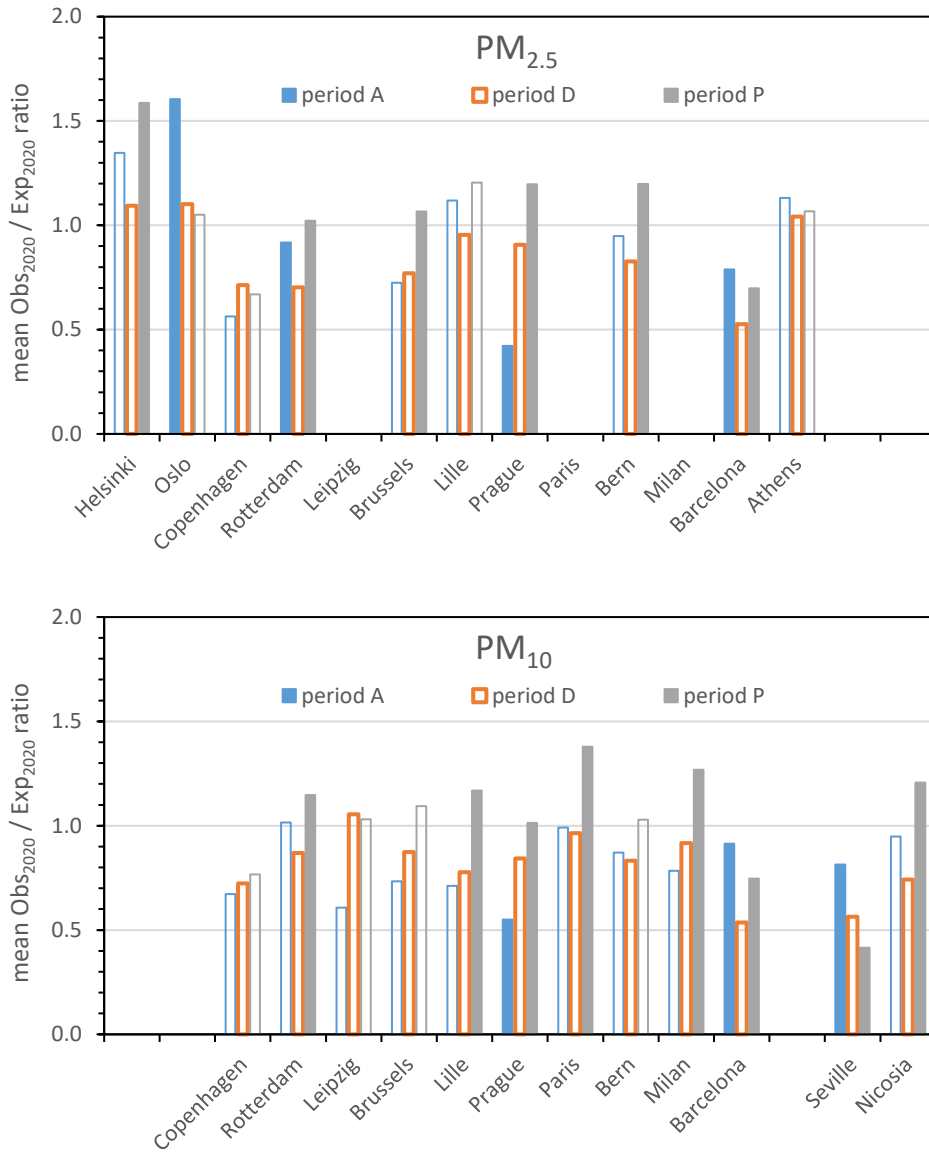
Figure 3. Mean observed / expected $PM_{2.5}$ (top) and PM_{10} (bottom) concentration ratios (Eq. 3) during periods A (before), D (during lockdowns) and P (after) at urban sites. Filled bars indicate means which are statistically different from the mean during lockdown periods (D).

665
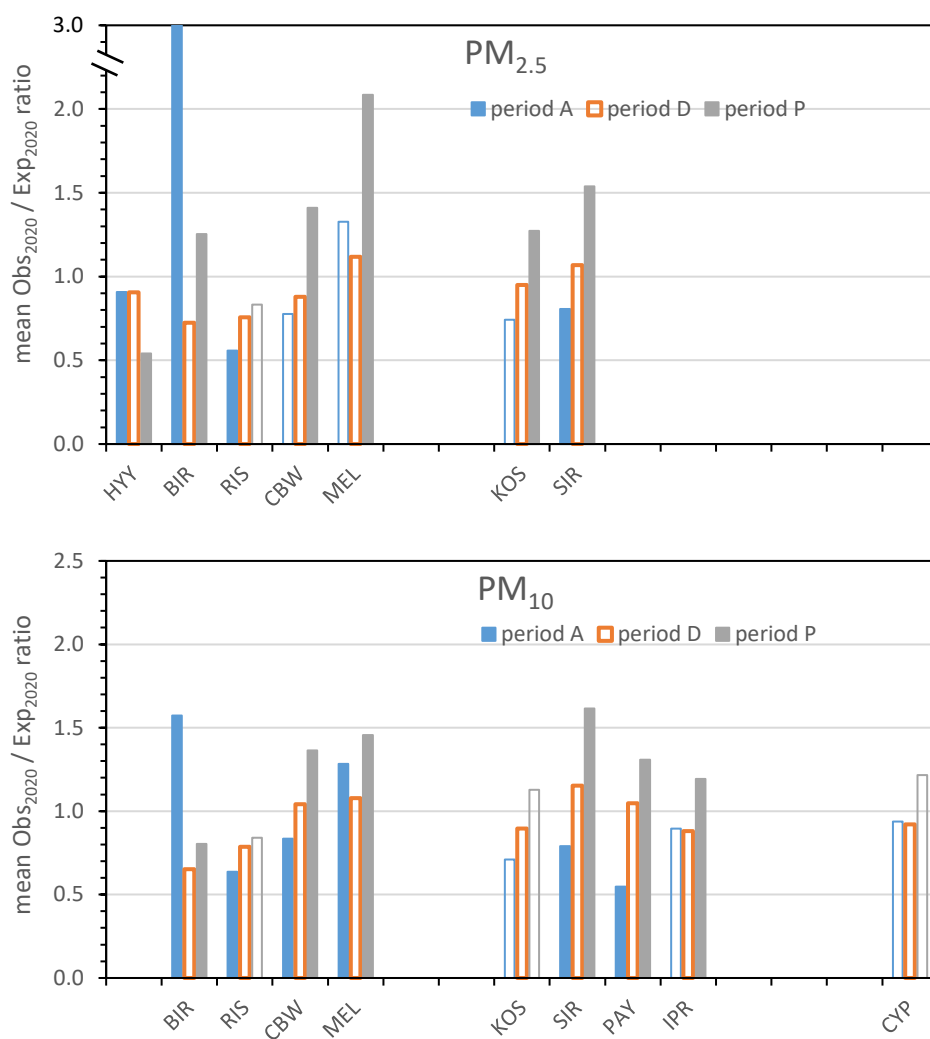
Figure 4. Mean observed / expected $PM_{2.5}$ (top) and PM_{10} (bottom) concentration ratios (Eq. 3) during periods A (before), D (during lockdowns) and P (after) at regional background sites. Filled bars indicate means which are statistically different from the mean during lockdown periods (D).
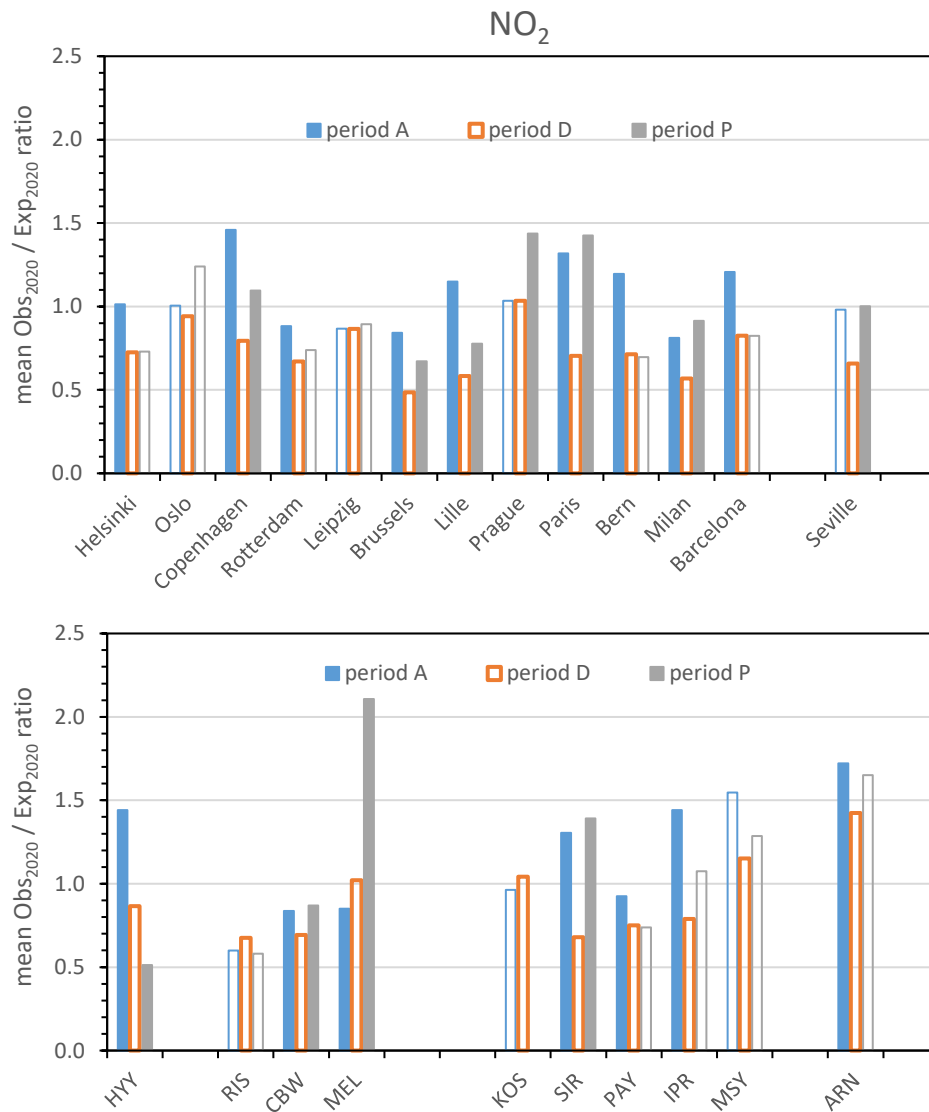
675

Figure 5. Mean observed / expected NO₂ concentration ratios (Eq. 3) during periods A, D and P. Filled bars indicate means which are statistically different from the mean during lockdown periods (D). No data available from KOS for time period P.
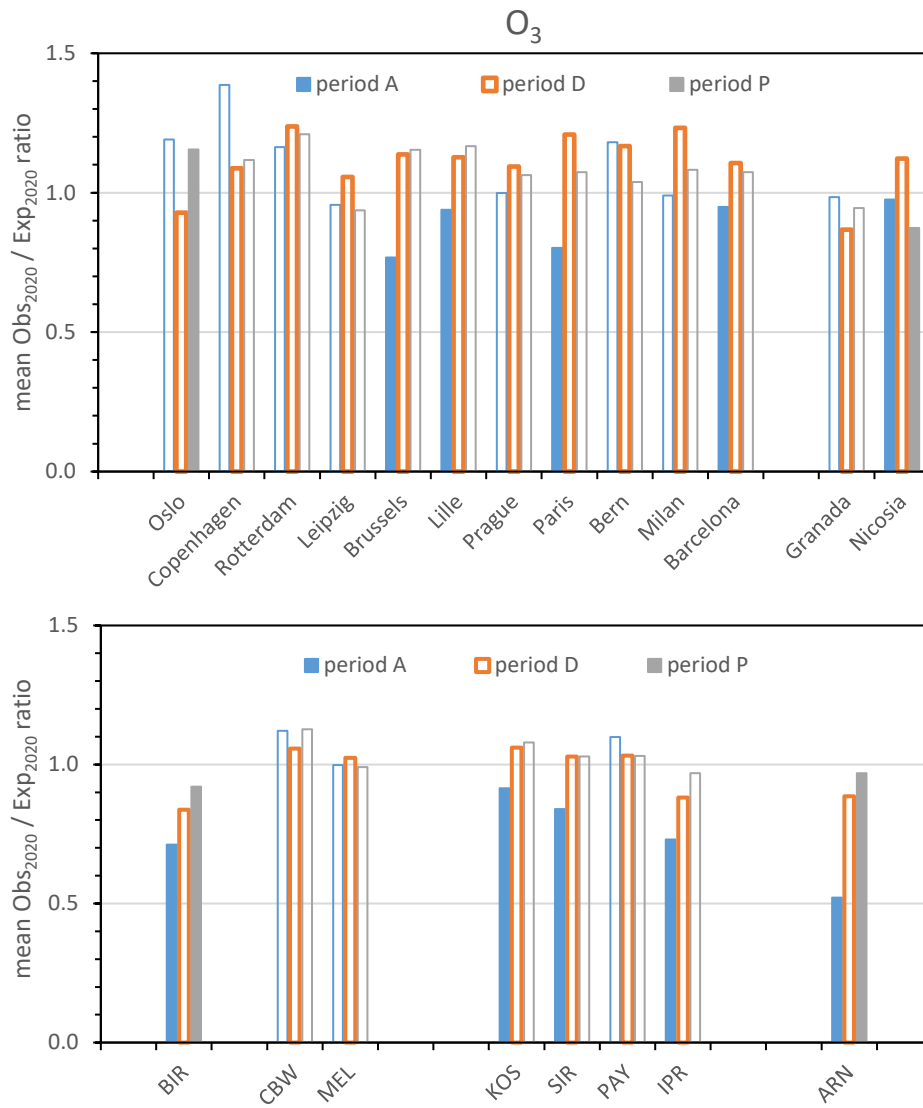
680

Figure 6. Mean observed / expected O_3 concentration ratios (Eq. 3) during periods A, D and P. Filled bars indicate means which are statistically different from the means during lockdown periods (D).
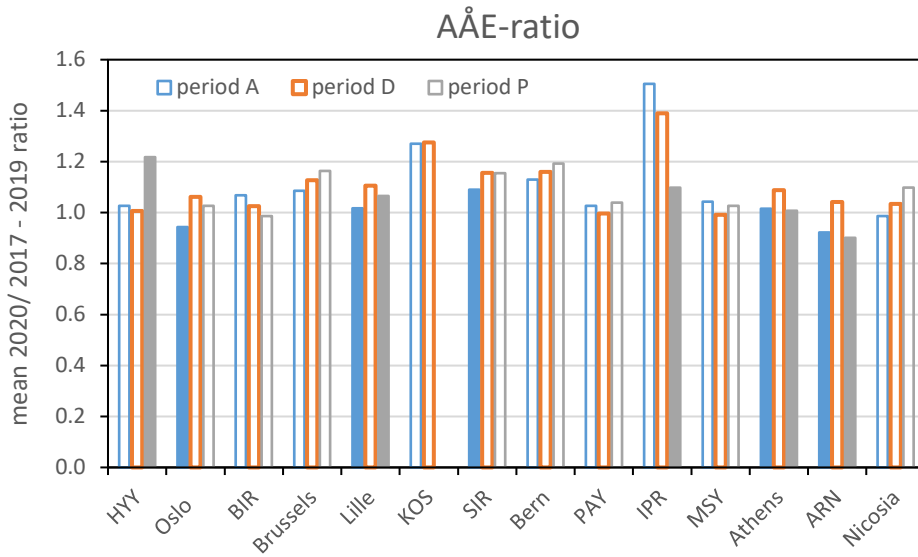
Figure 7. Mean 2020 / <2017 – 2019> AÅE ratios during periods A, D and P. Filled bars indicate means which are statistically different from the means during lockdown periods (D). No data available for KOS during period P.
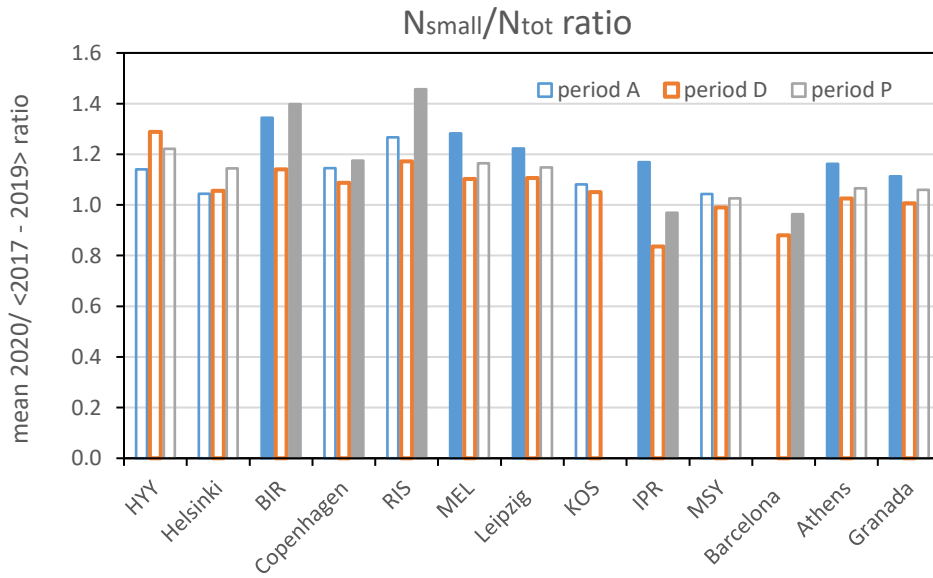
Figure 8. Mean 2020 / <2017 – 2019> N_{small} / N_{tot} ratios during periods A, D and P. Filled bars indicate means which are statistically different from the means during lockdown periods (D). No data available for KOS during period P, and for Barcelona during period A.

Table 1. Measurement site details.

	Urban sites				Regional background sites			
Country	Site	Type[1]	Latitude (°N)	Longitude (°E)	Site	Code	Latitude (°N)	Longitude (°E)
FI	Helsinki[2]	Background	60.19	24.95	Hyytiala	HYY	61.85	24.28
NO	Oslo	Background	59.92	10.77	Birkenes	BIR	58.39	8.25
DK	Copenhagen	Traffic	55.67	12.57	Risoe	RIS	55.64	12.09
NL	Rotterdam	Background	51.93	4.23	Cabauw	CBW	51.97	4.92
DE	Leipzig[3]	Background	51.32	12.30	Melpitz	MEL	51.53	12.93
BE	Brussels	Background	50.80	4.36				
FR	Lille	Background	50.63	3.09				
CZ	Prague	Background	50.01	14.45	Kosetice	KOS	49.57	15.08
FR	Paris	Background	48.89	2.35	SIRTA	SIR	48.71	2.16
CH	Bern	Traffic	46.95	7.44	Payerne	PAY	46.81	6.95
IT	Milan	Background	45.48	9.23	Ispra	IPR	45.82	8.64
ES	Barcelona	Background	41.39	2.12	Montseny	MSY	41.77	2.35
GR	Athens	Background	38.00	23.82				
ES	Seville	Background	37.35	-6.06	El Arenosillo	ARN	37.10	-6.73
ES	Granada	Background	37.16	-3.61				
CY	Nicosia	Background	35.14	33.31	Agia Marina	CYP	35.04	33.06

(1) "Background" and "Traffic" stand for "urban background" and "traffic" sites, respectively.
(2) Helsinki PNSD data are from the University of Helsinki science campus area located at 60.20 °N, 24.96 °E.
(3) Leipzig PNSD data are from the Leipzig Science Park area located at 51.35°N, 12.43°E.

Table 2. Mean impacts of the lockdown measures implementation and relaxation (%) as computed from the 2020 observed / expected ratios shown in Figures 2 to 8.

Variable	Site Type	Impact of lockdown measures			
		implementation		relaxation	
$PM_{2.5}$	Urban	+1 %	± 42 %	+26 %	± 21 %
	Regional background	+2 %	± 39 %	+38 %	± 43 %
PM_{10}	Urban	+5 %	± 33 %	+26 %	± 24 %
	Regional background	+15 %	± 42 %	+28 %	± 10 %
NO_2	Urban	-29 %	± 17 %	+31 %	± 30 %
	Regional background	-17 %	± 24 %	+27 %	± 50 %
O_3	Urban	+11 %	± 23 %	-3 %	± 12 %
	Regional background	+17 %	± 24 %	+4 %	± 5 %
AÅE	Urban	+7 %	± 4 %	0 %	± 5 %
	Regional background	0 %	± 7 %	-14 %	± 37 %
N_{small}/N_{tot}	Urban	-7 %	± 5 %	+6 %	± 2 %
	Regional background	-9 %	± 13 %	+11 %	± 12 %

695

700